

THESIS

BRUSH-LIKE SURFACE USING HEPARIN/CHITOSAN BASED NANOPARTICLES FOR  
BLOOD-CONTACTING APPLICATIONS

Submitted by

Rajvir Singh Nijjar

Department of Chemical and Biological Engineering

In partial fulfillment of the requirements

For the Degree of Master of Science

Colorado State University

Fort Collins, Colorado

Summer 2013

Master's Committee:

Advisor: Matt Kipper

Travis Bailey

Melissa Reynolds

## ABSTRACT

### BRUSH-LIKE SURFACE USING HEPARIN/CHITOSAN BASED NANOPARTICLES FOR BLOOD-CONTACTING APPLICATIONS

With increasing applications of biomedical implants, it is crucial to develop surfaces that are blood compatible, meaning they do not induce platelet or protein adhesion. Many implants that are currently used to treat a wide range of problems have one major drawback, they can induce thrombosis. The endothelial glycocalyx plays a crucial role in preventing thrombosis. Based on this idea, we set out to develop a surface that has a brush-like structure similar to that of the endothelial glycocalyx. We developed the surface by adsorbing negatively charged heparin/chitosan polyelectrolyte complex nanoparticles onto a heparin/tri-methylchitosan polyelectrolyte multilayer. The surface was then characterized using surface plasmon resonance (SPR), quartz crystal microbalance (QCM), atomic force microscopy (AFM), scanning electron microscope (SEM), and polarization modulation-infrared reflection absorption spectroscopy (PM-IRRAS). Using these techniques we confirmed that we had created a surface with brush-like structure. Our hypothesis that the nanoparticles on the surface swell and form a brush-like structure when exposed to physiological conditions seems to be correct, as a result, we feel the surface we have developed could have a wide range of applications in the biomedical field.

## ACKNOWLEDGEMENTS

This project would have not been possible without the support of many people. I would like to give many thanks to my adviser, Matthew J. Kipper, who gave me the opportunity of working in his lab and was there to answer all my questions. I would also like to thank Laura Place who helped me along the way with my project. And finally, I would like to thank my dad and mom, fiancée Karen, and numerous friends who endured the entire process with me, always offering support and love.

## TABLE OF CONTENTS

ABSTRACT.....	ii
ACKNOWLEDGEMENTS.....	iii
CHAPTER 1: INTRODUCTION.....	1
1.1 Motivation.....	1
1.2 Thrombosis.....	2
1.2.1 Mechanism of thrombosis.....	2
1.3 Endothelial glycocalyx and its composition.....	4
1.4 Heparin and anti-thrombosis.....	8
1.5 Blood compatible surfaces.....	10
1.5.1 Heparin-based surfaces.....	11
1.5.2 Glycocalyx-mimetic surfaces.....	12
1.6 Glycocalyx-mimetic surfaces using polyelectrolyte complex nanoparticles.....	16
CHAPTER 2: EXPERIMENTAL SECTION.....	20
2.1 Materials.....	20
2.2 Construction of heparin/chitosan polyelectrolyte complex nanoparticles.....	20
2.3 Preparing the Hep, Tmc, Chi, and fibrinogen solutions for construction of PEM.....	21
2.4 PEM assembly and in situ Fourier-transform surface plasmon resonance.....	22
2.5 Scanning electron microscopy.....	24
2.6 Atomic force microscopy.....	24
2.7 Multilayer assembly using quartz crystal microbalance.....	24
2.7.1 Kelvin-Voigt viscoelastic modeling for PCN-coated surface.....	25
2.8 Polarization modulation-infrared reflection adsorption spectroscopy.....	28
CHAPTER 3: RESULTS AND DISCUSSION.....	30
3.1 Background.....	30
3.2 Formation of PEMs and PCN-coated surface using surface plasmon resonance.....	30
3.3 Surface morphology.....	34
3.4 Surface chemistry.....	36
3.5 Formation of PEMs and PCN-coated surface using quartz crystal microbalance.....	39
CHAPTER 4: CONCLUSION.....	46

4.1 Conclusion.....	46
REFERENCES .....	47

## CHAPTER 1

### INTRODUCTION

#### 1.1 MOTIVATION

The applications of artificial implants and blood-contacting devices have grown significantly over the past fifty years [1]. As a result of the advances made in the biomedical field in regards to these devices, people have been able to live out more comfortable lives. The medical field makes extensive use of blood-contacting devices to treat a wide range of diseases from cardiovascular disease to kidney failure. For example, 200 million catheters per year, 4 million stents per year, and 1.2 million artificial kidneys per year are used worldwide [2]. Devices that are in contact with blood have the potential to induce thrombosis, inflammation, and infection. These three processes are the greatest limitations to the long term success of the aforementioned devices and many others [3]. To put the failure rate into perspective, over 550,000 vascular grafts are implanted each year in the United States and of those only 15 to 40% are successful; the underlying causes of failure are thrombosis, inflammation, and infection [4]. Conventional methods such as anti-coagulants and antibiotic therapy have proved to be ineffective [3, 4]. If blood-contacting materials can overcome thrombosis, inflammation, and infection then they have the potential to be used in numerous biomedical applications.

To improve the long-term success of implants focus has now shifted to developing surfaces that are blood-compatible. It is now believed that surface properties play a huge role in the generation of thrombosis, inflammation, and infection [4]. In particular, it is believed that the endothelial glycocalyx plays a significant role in preventing thrombus formation in blood vessels [5, 6]. Using the endothelial glycocalyx as the model, the goal of this project is to develop and characterize a brush-like surface composed of heparin-chitosan nanoparticles that mimics the

glycocalyx with the intent of it being used as a surface coating to improve patency of biomaterials.

## 1.2 THROMBOSIS

To design implants and blood-contacting devices that are successful in the long term without the use of anticoagulants or antithrombotic drugs, effort needs to be made to understand how synthetic biomaterials affect mechanisms of thrombosis, inflammation, and infection. Blood circulation is a closed loop that carries vital nutrients throughout the body. In the event of an injury the body reacts by forming a clot (thrombus) which seals the damaged site and prevents further blood loss. Therefore, thrombus formation is an essential process that helps maintain the integrity of the circulatory system. The body's response in dealing with foreign materials is very similar to the way it deals with injuries to the circulatory system. Thus, it is crucial to understand these mechanisms. Extensive research has been done in regards to the mechanisms involved in blood clotting but it still presents challenges, in particular the role that white blood cells play in coagulation [2]. Current research focuses on the role that surface-adsorbed proteins play in activating blood coagulation. Proteins that adsorb to the surface of biomaterials are believed to activate platelets, resulting in further platelet adhesion and finally leading to thrombosis and activation of coagulation cascade [5, 7].

### 1.2.1 MECHANISM OF THROMBOSIS

The first step in the formation of thrombus in the event of vessel injury is the activation and adhesion of platelets. At the site of injury, platelets in the blood are exposed to collagen in the sub-endothelial matrix. Receptors on the outer membrane of platelets, glycoprotein VI and glycoprotein Ib, mediate the adhesion between the platelets and collagen [6, 8]. Adhesion can also be mediated by integrins  $\alpha_2\beta_1$  and  $\alpha_{IIb}\beta_3$  which bind to collagen and fibrinogen [6, 8]. It is

believed that the binding of these proteins to the surface of blood-contacting surfaces is likely the first step in the adhesion of platelets to the surface of implants. The consequence of platelet adhesion further leads to thrombus formation or the inflammatory response.

Thrombus formation is also accompanied by blood coagulation. Blood coagulation is a cascade that produces thrombin which converts fibrinogen into fibrin, the key component in stabilizing the clot. The cascade is composed of two separate pathways that ultimately lead to the formation of thrombin: the intrinsic pathway and the extrinsic pathway [8, 9]. The intrinsic pathway is activated within the first 100-200 s of initial contact between the surface and the blood [8]. The intrinsic pathway does not play as significant of a role as the extrinsic pathway in blood vessels.

The extrinsic pathway involves the exposure of tissue factor (TF) to blood. TF is located in the adventitial and medial tissue layers of blood vessels [8]. The exposed TF interacts with factor VII to form activated factor VII. This activated factor VII then goes on to cleave factor X to form activated factor X. The activated factor X then interacts with factor V to form activated factor V. This interaction from the activated factor X and activated factor V complex has the ability to convert prothrombin to thrombin. Thrombin can now convert fibrinogen to fibrin, the key component that stabilizes a clot by forming a cross linked network. It was originally believed that tissue factor was located on the surface of blood vessels but evidence suggests that TF also circulates in the blood, secreted by monocytes and neutrophils [8]. This is a very important finding because it suggests that tissue factor from the blood binds to surfaces and activates the coagulation cascade.

Thrombosis is an important response by the body necessary for homeostasis. But, when it comes to the long-term success of cardiovascular implants such as vascular grafts, stents, heart

valves, and vascularized tissues and organs, we need to be able to shut down thrombosis on these surfaces. Such a surface does exist, the endothelium has the ability to inhibit adhesion and activation of platelets, block the coagulation process, and mediate clot dissolution [8]. Being able to understand the mechanisms involved in thrombosis allows one to engineer surfaces that mimic the endothelium.

### 1.3 ENDOTHELIAL GLYCOCLYX AND ITS COMPOSITION

The glycocalyx is an important constituent of the endothelium; it is believed to impart anti-thrombogenic properties to the vessel walls [2]. As shown in figure 1, it is located on the luminal side of all blood vessels and has a brush-like structure that is composed of glycoproteins, proteoglycans, glycosaminoglycans (GAG) and associated plasma proteins. It has an overall negative surface charge due to hyaluronic acid and heparan sulfate. Due to the negative surface charge the glycocalyx is extremely hydrophilic. Studies show that surfaces that are hydrophilic tend to resist non-specific protein adsorption compared to more hydrophobic surfaces [3, 5, 6, 10, 11]. This is a result of water binding so strongly to the surface that it cannot be displaced by the proteins. The thickness of the glycocalyx was believed to be on the order of nanometers but new evidence suggests that it can reach up to 0.5-3  $\mu\text{m}$  [6, 12]. Any injury to the glycocalyx exposes the endothelium which rapidly leads to thrombosis [8]. This has caused researchers to shift their focus in studying the role that glycocalyx plays in thrombosis.

Aside from the surface chemistry of the glycocalyx, studies have shown that surface characteristics such as surface roughness also play a role in giving the glycocalyx its anti-thrombogenic properties. Shear rate or shear stress is an important factor in determining which platelets adhere to it. At low shear stress, proteins adhere to fibronectin, vitronectin or fibrinogen. At medium shear rates adhesion is mainly due to fibrinogen and at high rates vWF

(von-Willebrand factor) is favored [9]. Some studies have shown that at low shear rates vWF circulates in the blood as a spheroid like shape whereas at very high shear rates it is in a linear chain conformation. This conformation at high shear rates makes vWF 50 times more likely to bind to the surface of a foreign body or injured endothelia, and as a result, platelets mainly bind to vWF at high shear stress [9]. The walls of the endothelium are constantly exposed to mechanical forces; some studies suggest that the glycocalyx is in part responsible for the translation of biomechanical forces into biochemical signals [6, 13]. Thus is it important to take into consideration how the surface will affect the sheer rate when designing surfaces that are in contact with blood.

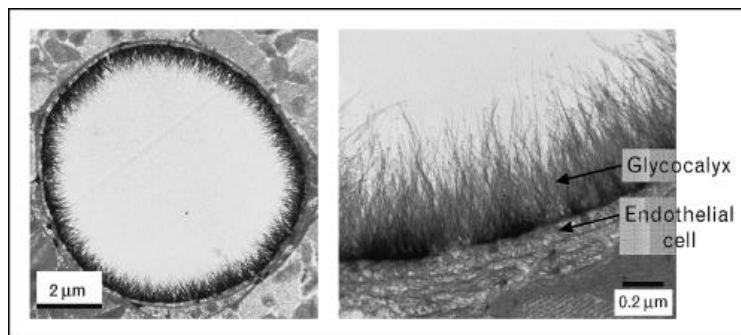


Figure 1. Electron microscopy image of the endothelial glycocalyx in a coronary capillary [12]. Current opinion in lipidology by LIPPINCOTT WILLIAMS & WILKINS, INC.. Reproduced with permission of LIPPINCOTT WILLIAMS & WILKINS, INC. in the format reuse in a dissertation/thesis via Copyright Clearance Center.

As mentioned before surface charge is an important factor in determining the adhesion properties of a surface. Surfaces that are hydrophilic tend to resist protein/bacterial adhesion compared surfaces that are hydrophobic. Several groups have done studies to show the correlation between bacterial adhesion and surface hydrophilicity/hydrophobicity. For example, Ludwicka et al. did studies to show how different strains of *S. epidermidis* interact with different synthetic polymers. They concluded that increasing negative surface charge, which also increased the hydrophilicity of the surface, resulted in a decrease in bacterial adhesion [3]. Other groups have shown that hydrophobic surfaces adsorb more proteins, and as a result induce more

conformational changes in the adsorbed proteins. These conformational changes can then promote the inflammatory response as well as further cell adhesion and blood platelet adhesion [11].

A new class of surfaces developed using polymer brushes have gained considerable attention due to their hydrophilic nature [5]. These surfaces have several advantages. They are hydrophilic, but more importantly their structure closely resembles that of the glycocalyx. This brush-like structure is very advantageous because not only can it resemble the glycocalyx, but there is also the possibility of conjugating biologically active molecules to the brush [5]. Several groups have successfully been able to create this brush-like surface using either grafted polymer chains or nanoparticles [5, 14-18]. These will be discussed in more detail later.

Surfaces that are now being developed all have one element in common: they try to mimic the surface of the endothelial glycocalyx in some fashion. The most promising types of surfaces are those that try to imitate the anti-thrombogenic nature of the glycocalyx. The glycocalyx is inherently anti-thrombogenic. Injury to the glycocalyx exposes the endothelium which results in rapid thrombosis. Understanding the composition of the glycocalyx is the first step in understanding why the luminal surfaces of vessels are so anti-thrombogenic.

The endothelial glycocalyx is a carbohydrate-rich layer lining the luminal surface of blood vessels. It is linked to the surface through proteoglycans and glycoproteins. Due to the constant interaction with plasma this layer is in dynamic equilibrium with the components in blood and as a result it has variable thickness and composition [6]. The glycocalyx was first mentioned over 60 years ago but researchers are still having great difficulty in defining it geometrically. This problem arises from the fact that the glycocalyx suffers from enzymatic or shear-induced shedding [6, 13, 19]. The proteoglycans are considered to be the major

constituents of the glycocalyx, they are composed of syndecans and glypicans which are firmly bound to the surface and mimecan, perlecan, and biglycan which diffuse from the glycocalyx to the blood stream. Proteoglycans are linked to glycosaminoglycan chains of various lengths. It should be noted that proteoglycans are characterized by long un-branched side chains whereas the attached GAGs are short and branched. The glycosaminoglycan chains are what give the glycocalyx the brush-like structure. A simplified schematic (figure 2) shows the structure of the glycocalyx. Embedded in the glycocalyx is a wide range of enzymes, receptors and proteins that work together to regulate leukocyte and thrombocyte adhesion.

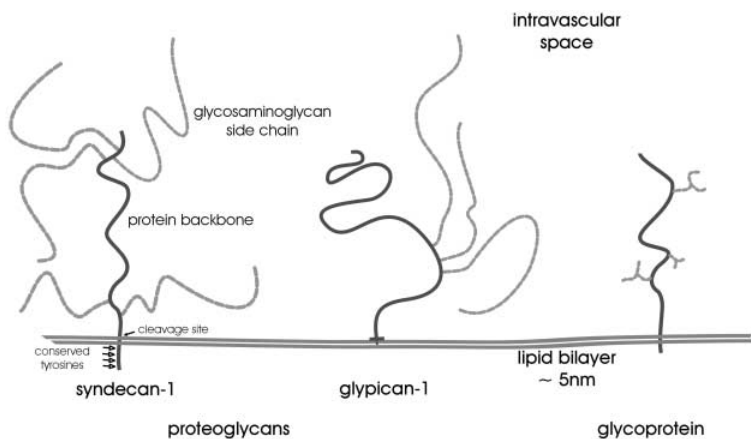
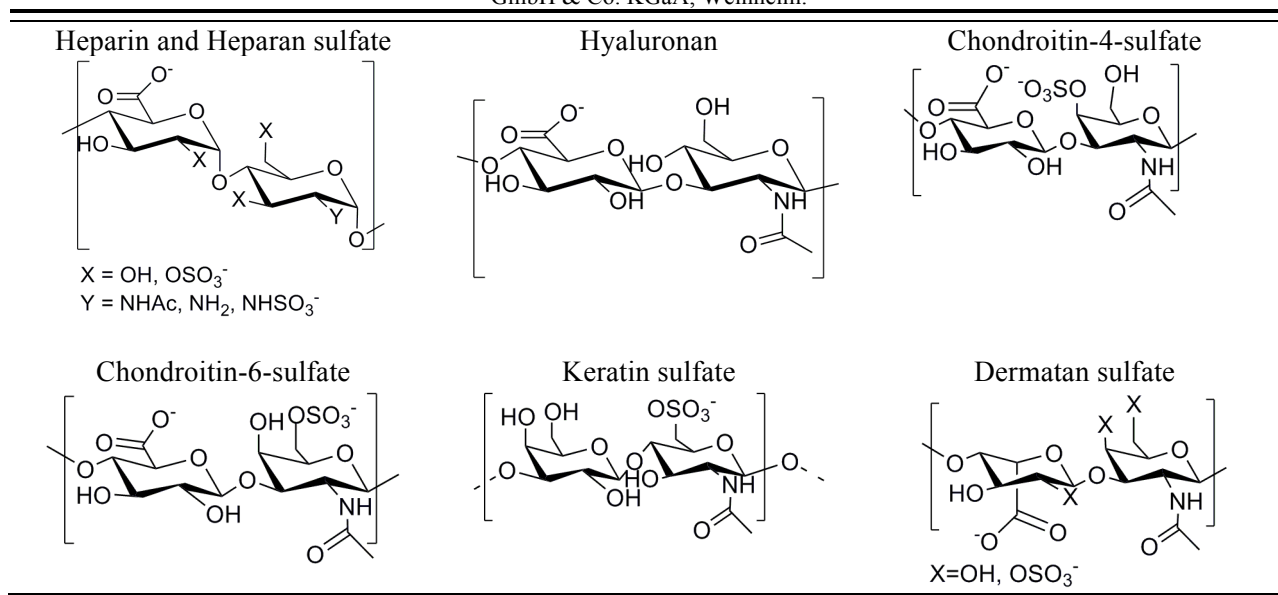


Figure 2. Simple schematic showing the glycoalyx. Syndecan and glypican are the main proteoglycans to which the glycosaminoglycans link to form the mesh like structure [19]. Pflügers Archiv : European journal of physiology by SPRINGER-VERLAG. Reproduced with permission of SPRINGER-VERLAG in the format use in a thesis/dissertation via Copyright Clearance Center.

The GAG side chains are a major contributor to the overall function of the glycocalyx. Five types of glycosaminoglycan chains are of special interest: chondroitin sulfate, dermatan sulfate, keratin sulfate, heparan sulfate, heparin, and hyaluronan [6, 19, 20]. These five GAGs are all very similar in composition in the sense that they are all composed of linear polymer chains of varying length with repeating disaccharide units containing uronic acid and hexosamine [6, 20, 21]. The chemical structure of the various GAGs is shown in table 1. Out of these five, three are of great importance: heparan sulfate, chondroitin sulfate/dermatan sulfate

and hyaluronan. In particular, heparan sulfate because it constitutes roughly 50-90% of the total composition of proteoglycans making up the glycocalyx [6, 12, 20, 21]. GAGs are able to interact with plasma-derived proteins through numerous specific binding sites. What is also remarkable about GAGs is how easily they can be modified; simple chain modifications can have great functional consequences. The fact that GAGs can be easily modified to give enormous structural diversity to similar length chains, leads to a wide array of biological functions. The most common modifications are *N*-sulfonation and *O*-sulfonation [6, 22, 23]. The numerous sulfation patterns and their effect on specific protein binding and modulation of protein function suggests that any process that alters the thickness of the endothelial glycocalyx could be responsible for modulating surface permeability as well as specific protein binding and activity.

Table 1. The Chemical structure of glycosaminoglycans found throughout the body [20]. Copyright © 2010 WILEY-VCH Verlag GmbH & Co. KGaA, Weinheim.



#### 1.4 HEPARIN AND ANTI-THROMBOSIS

Like mentioned before, the composition of the proteoglycans on the surface of glycocalyx is 50-90% heparan sulfate. Heparan sulfate plays an integral part in providing the

glycocalyx its anti-thrombogenic properties. It has been known for quite some time that heparan sulfate serves as a cofactor of anti-thrombin III (AT-III) which acts to inhibit thrombin. AT-III is a glycoprotein that is a major serine protease inhibitor. It inhibits some of the key components in the coagulation cascade such as thrombin, factor Xa, IXa, and XIIa. AT-III inactivates these proteases by trapping them and forming a 1:1 stoichiometric complex. This results in them not being able to access their substrates [24]. The interaction between AT-III and thrombin is thought to be a result of interactions between the protease and a specific reactive peptide bond within AT-III [25]. Thrombin in an attempt to attack the reactive peptide bond within AT-III, activates AT-III and becomes trapped. This leads to an inactive anti-thrombin-protease complex. The formation of anti-thrombin-thrombin complex has been shown to occur at a relatively slow rate but the presence of heparin has been shown to accelerate this interaction significantly [25]. Several studies have shown the significant effect that heparin has on anti-thrombin by studying the change in rate constants in the presence of heparin and without heparin. Without heparin, the rate constants for thrombin, factor XA and factor IXa inactivation are  $7-11 \times 10^3$ ,  $2.5 \times 10^3$  and  $1 \times 10 \text{ M}^{-1}\text{s}^{-1}$  respectively whereas in the presence of heparin the rate constant jumps to  $1.5 -4 \times 10^7 \text{ M}^{-1}\text{s}^{-1}$  [24, 26-30]. As can be seen, the presence of heparin has a significant effect on the inactivation of the aforementioned thrombin inducing factors. To put it into perspective, the reaction for anti-thrombin-thrombin reaction is increased by 2000-4000 fold.

Anti-thrombin activity is significantly increased when it interacts with two specific domains on heparin. The first domain consists of eight or more oligosaccharide sequences, this domain binds to a discrete region in anti-thrombin to increase factor Xa-AT-III interactions [25]. The second domain which is responsible for thrombin inactivation contains polysaccharides that

are 16 or more residues [25]. Do to the effect of heparin on AT-III future technologies are focused on developing surfaces that incorporate heparin in some fashion.

Like mentioned earlier, the mechanisms for thrombus formation are clearly understood but what is still somewhat unclear is how foreign surfaces alter the coagulation pathway. Many groups have come to the consensus that the endothelial glycocalyx is a key component in regulating the blood-clotting cascade in particular the heparan sulfate. For this reason many surface modifications incorporate heparin on their surfaces. Heparin has been used as an anti-coagulant for quite some time now, but it has limitations. Once the implant is inserted in the patient heparin must be administered on a regular basis. The down side of using heparin in anticoagulation therapy is the potential of forming heparin-induced thrombocytopenia. This results when heparin, which has a negative charge, forms a complex with positively charged platelet factor 4 (PF4). This complex then becomes the target of the immune system with the final outcome being venous and arterial thrombosis [31, 32]. Adverse reactions like these have caused researchers to look for alternative techniques to deal with surface-induced thrombosis.

### 1.5 BLOOD COMPATIBLE SURFACES

The problem of developing a truly blood compatible surface is being investigated by countless groups around the world. Great progress has been made in this field but a lot more work needs to be done before there are truly blood-compatible surfaces. This all stems from not fully understanding how biomaterials interfere with the coagulation cascade. Groups have taken advantage of how heparan sulfate on the surface of endothelial cells interacts with anti-thrombin to develop heparin coated surfaces that show great potential [28, 30, 33]. Other groups have tried to make surfaces that mimic the structure of the glycocalyx with the hypothesis that surface

topography is equally as important as is the chemistry [10, 14]. Studies relating to surface topography will be closely examined.

### 1.5.1 HEPARIN-BASED SURFACES

To improve the compatibility of surfaces a common technique is to coat the surface with heparin. Many studies have been done to show that surfaces coated with heparin are more likely to resist platelet adhesion. Many of the biomedical devices that are in use today are made using titanium; titanium is a very good starting material for biomedical devices because of its properties such as low modulus and corrosion resistance. But the down side of titanium is that it is very thrombogenic compared to other biomaterials. Chen et al. have shown that coating titanium with heparin multilayers improves their blood compatibility [33]. They coated titanium surfaces using a layer by layer (LbL) technique. This technique involves coating the surface with oppositely charged polyelectrolytes that are then alternatively adsorbed on to the surface. LbL is very flexible in that it allows one to control the layer thickness down to the nanometer scale, and it is not limited by shape of surfaces. Chen et al. used heparin-collagen multilayers on titanium to improve the blood compatibility of titanium cardiovascular implants. They exposed titanium surfaces to platelets and compared them to surfaces coated with heparin-collagen multilayers. Using SEM they observed that both surfaces adsorbed platelets but the heparin-collagen adsorbed about half the amount as the titanium surfaces. They also observed that the platelets on the heparin-collagen surfaces were not activated platelets. Two additional anticoagulant assays were performed, the activated partial thromboplastin time (APTT) and the prothrombin time (PT) tests. These two tests measure the time activity of the intrinsic and common pathway of blood coagulation. The study showed that the APTT and PT for untreated titanium were  $49.2 \pm 3.8$  s and  $18.8 \pm 0.8$  s respectively whereas surfaces coated with heparin-collagen the APTT and

PT were  $132.8 \pm 14.9$  s and  $35.3 \pm 6.0$  s respectively [33]. This study showed that coating surfaces with heparin is an effective technique of improving the blood compatibility of surfaces.

### 1.5.2 GLYCOCALYX-MIMETIC SURFACES

The multilayer technique shows great promise in treating biomaterial-induced thrombosis but researchers have taken it a step further by trying to design polymer-based brush-like surfaces that they believe will mimic the glycocalyx. Multiple groups have approached this problem and have come up with several techniques to design these surfaces. Some groups have tried to design these surfaces by grafting polymer chains on to surfaces with varying densities whereas other groups have used nanoparticles to achieve similar brush-like surfaces [10, 14]. Both types will be discussed in detail.

Grafting polymer chains on to surfaces to mimic the glycocalyx has gained considerable attention in regards to preventing biomaterial-induced thrombosis. Several different polymers have been used in this application ranging from natural polysaccharides to poly(ethylene glycol) (PEG). Gupta et al. set out to create a glycocalyx-mimetic surface using dextran modified poly(vinyl amine) [10]. The advantage of poly(vinyl amine) (PVA) is that it adsorbs to a wide range of biomaterial surfaces spontaneously [10]. The chemical structures of both PEG and PVA is shown in figure 3. They successfully designed the surface and performed various tests to see whether the surface was able to resist platelet adhesion, as well as testing for the stability of the surface. The schematic of the surface they were trying to achieve is shown in figure 4. An important property of the surface is how stable it is, if the surfaces starts to shed under sheering then there is the potential that the exposed surface will allow platelet adhesion. They checked the stability of the surface by fluorescently labeling the surface and then exposing it to flowing blood. They observed that there was no change in the intensity before and after exposure to

whole blood indicating that the brush-like structure was stable. They also performed platelet adhesion studies under various shear stress conditions ranging from 0 dyne/cm<sup>2</sup> to 80 dyne/cm<sup>2</sup>. Their studies showed that uncoated surfaces had roughly 35,000 adhered platelet number/mm<sup>2</sup> at no shear and this value drops below 10000 adhered platelet number/mm<sup>2</sup> at shear stress above 60 dyne/cm<sup>2</sup>. For surfaces coated with poly(vinyl amine) they observed that the adhered platelets number/cm<sup>2</sup> never goes above 5000 and stays relatively constant regardless of an increase in shear stress [10].

Currently PEG is used as the benchmark for reducing protein adsorption and platelet adhesion on blood-contacting materials but the chain length, surface density, and surface heterogeneity play a crucial role in determining the surface properties of PEG which affect the repulsion barrier. Gupta et al. believe that PVA will overcome these, because unlike PEG oligosaccharides have no amphiphilic or surface-active characteristics [10]. They believe that PVA is superior to PEG; the only difficult part about PVA is getting a dense uniform coverage on the surface. Do to the inherent properties of PEG a low surface density still allows it the ability to be able to spread over the surface. PVA on the other hand cannot get away with a less dense packing because this exposes the surface underneath, allowing platelet adhesion. According to Gupta et al. there is a huge variability between surfaces coated with dextran that is oriented “end on” and “side on”. The variability can be reduced to nothing if the packing density can be increased significantly. The advantage that PVA has over PEG is that it will not undergo interfacial dehydration under dense packing. They are successful in their attempt to make a densely packed surface by modifying the dextran so that it has more sites for binding the surface. This enables them to create a surface with a dense packed surface of dextran modified poly(vinyl

amine) that resembles the brush-like structure of the glycocalyx. This surface was shown to reduce platelet adhesion by 90% compared to non-coated surfaces [10].

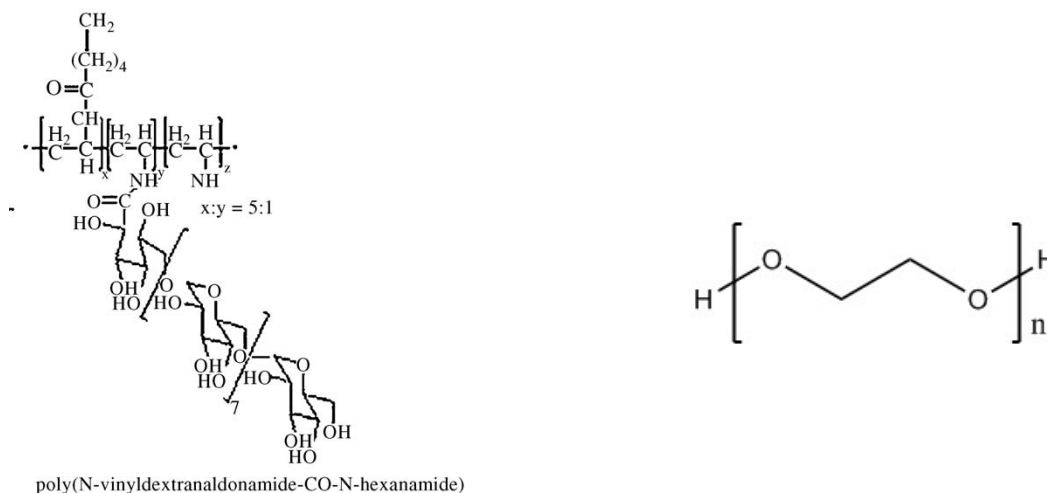


Figure 3. The chemical structure of PVA (left) and PEG (right). Biomaterials by Biological Engineering Society Reproduced with permission of PERGAMON in the format reuse in a thesis/dissertation via Copyright Clearance Center.

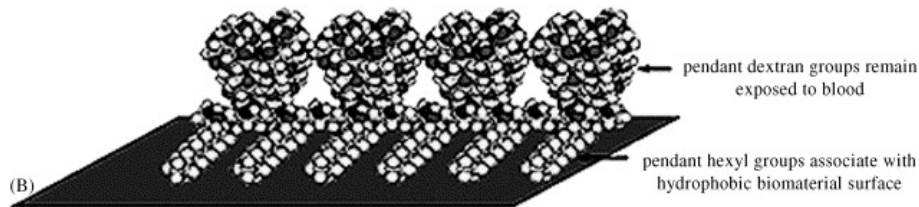


Figure 4. Schematic of glycocalyx-mimetic surface using dextran-modified poly(vinyl amine) [10]. Biomaterials by Biological Engineering Society Reproduced with permission of PERGAMON in the format reuse in a thesis/dissertation via Copyright Clearance Center.

Several groups have created these brush-like surfaces using various polymers. They all have one goal in mind and that is to create a high density brush-like surface that mimics the glycocalyx in terms of anti-thrombogenicity [15-17]. The starting material for a lot of these surfaces is simple carbohydrates. Yu et al. designed glycopolymer brushes using mannose, galactose and glucose residues in the pyranose form [5]. The reason for using carbohydrates is because they are abundantly present on the surface of the endothelial glycocalyx. This group was also able to show that their surface was able to resist platelet adhesion. Another important

finding of their study was that brush surfaces based on glucose adsorbed lower amount of protein than the mannose or galactose brushes [5]. These studies also confirmed that brush density is a critical factor in protein adsorption. Many groups have been able to graft polymer chains on the surface of various biomaterials but the challenge lies in getting a very dense coating.

While some groups have managed to graft polymer chains onto surfaces to mimic the glycocalyx others have approached the problem from another perspective. Instead of grafting polymer chains onto surfaces some groups have resorted to binding nanoparticles onto surfaces. The end goal is the same for both techniques, to obtain a brush-like surface that has the potential to mimic the glycocalyx. Barrientos et al. set out to create a surface using gold glyconanoparticles that has the potential to be used for a wide range of applications in the biomedical field [14]. They developed their nanoparticles by using a gold sphere core with neoglycoconjugates of naturally occurring oligosaccharides bound to the entire outer surface thus, giving a globular shape. When they form clusters on the surface they resemble the brush-like structure that is so sought after. Figure 5 shows a simple schematic of how this group attempted to create this brush-like surface. One of the main objectives of this group was to develop a surface that was resistant to cell-adhesion processes, to achieve this objective they wanted to make sure that their surface was stable in regards to enzymatic degradation. They believed that the steric crowding of the carbohydrate groups on the surface would allow it to go undetected by degradation enzymes [14]. This is exactly what they observed experimentally; highly dense nanoparticles were able to resist hydrolysis by  $\beta$ -galactosidase whereas less dense nanoparticles were hydrolyzed.

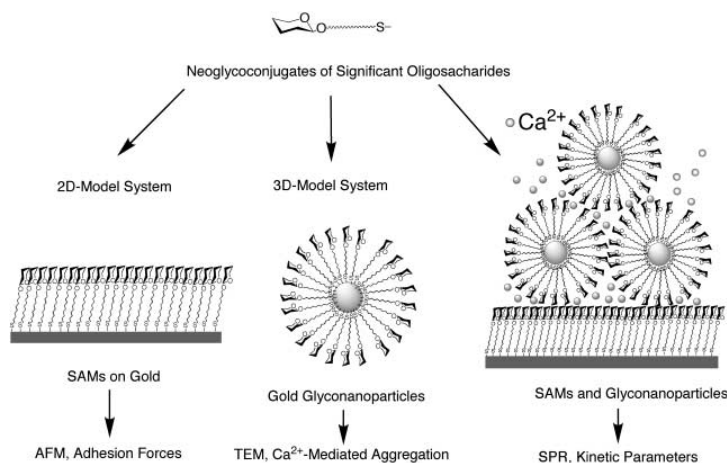


Figure 5. Scheme for making brush-like surfaces using gold glyconanoparticles [14]. Chemistry : a European journal by Gesellschaft Deutscher Chemiker ; et al Reproduced with permission of WILEY - V C H VERLAG GMBH & CO. KGAA in the format reuse in a dissertation/thesis via Copyright ClearanceCenter.

## 1.6 GLYCOCALYX-MIMETIC SURFACES USING POLYELECTROLYTE COMPLEX NANOPARTICLES

While surfaces made using polymer brushes and surfaces made using nanoparticles show great promise there has not been a lot of work done in regards to obtaining brush-like surfaces using nanoparticles. Much of the work reviewed above is focused on using polymers such as PVA and PEG to create brushes. Like mentioned before, the major problem when grafting polymer chains on to surfaces is obtaining a uniform and dense coverage. Without a dense coverage the underlying surface is exposed to blood and therefore is much more prone to platelet adhesion. It has been already shown by several groups that we can engineer surfaces that have somewhat a brush-like structure using polymer chains but very few groups have explored the idea of obtaining brush-like surfaces using clustered nanoparticles.

The idea behind using clustered nanoparticles as opposed to grafting polymer chains is very appealing because it is easier to get a uniform coverage of the surface using nanoparticles than using grafted polymer chains. In particular, nanoparticles synthesized using polyelectrolyte polysaccharides are of great significance. These nanoparticles have a significant advantage in

that they are made using the same GAGs found on the endothelial glycocalyx, heparin. Previous work done in our lab has been able to develop surfaces using nanoparticles but their potential as protein resisting surfaces was never explored [34].

It has been known for quite some time now that when two polyelectrolytes are mixed in solution they form colloiddally stable polyelectrolyte complex nanoparticles (PCNs). Work done by Boddohi et al. has shown that mixing two different polyelectrolyte polysaccharides will result in the formation of PCNs [35]. In his work he was able to create various combinations of PCNs. The formation of stable PCNs is obtained when two oppositely charged polyelectrolytes are mixed in non-stoichiometric amounts. The PCNs carry a charge depending on which polyelectrolyte was used in excess. This allows for the creation of PCNs with either an overall positive or negative charge depending on the application. For applications for anti-thrombogenic surfaces we are going to use PCNs that are made using heparin and chitosan which will have an overall negative charge. When these PCNs are exposed to PEMs made using polyelectrolyte polysaccharides they attach through charged interactions. For example, if the PCNs are of negative charge then they will bind to multilayers that are positively terminated and vice versa. The final shape of the PCNs can vary depending on how big of a difference there is in the molecular weights of the polyelectrolytes used. The two different conformations can be seen in figure 6. Unlike other nanoparticles, PCNs made using polyelectrolyte polysaccharides have an additional advantage in that they are water soluble making them perfect for use in biomedical applications.

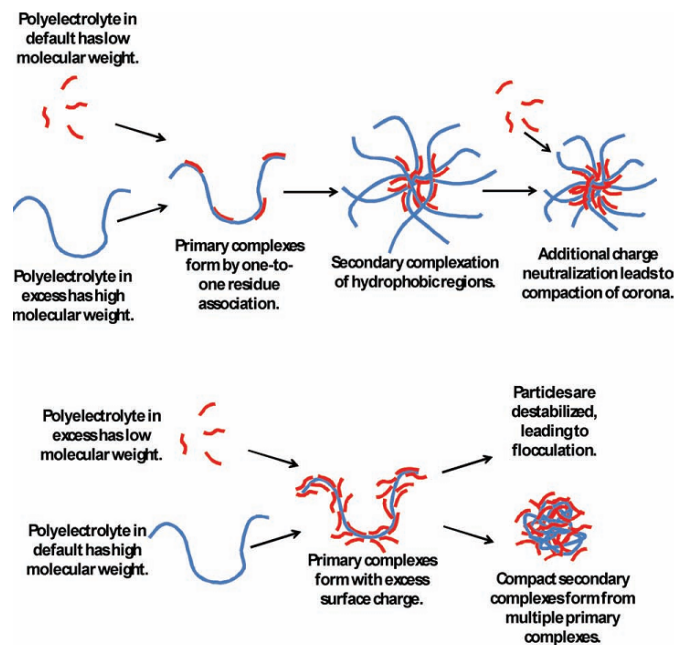


Figure 6. Formation of PCN using polyelectrolytes with significantly different molecular weight [20]. Copyright © 2010 WILEY-VCH Verlag GmbH & Co. KGaA, Weinheim.

Previous work has shown that these nanoparticles are able to bind to the surface but no work has been done regarding its ability to resist platelet and protein adhesion [34]. As previously mentioned, the goal of this project is to take the surface that has been previously developed and see whether or not it has the potential to be anti-thrombogenic. Gold substrates will be used on which multilayers of heparin and trimethyl-chitosan (Tmc) will be formed. The PEMs give a solid foundation on which the negatively charged heparin/chitosan particles can bind. The hypothesis is that once the surface is exposed to physiological conditions the PCNs will swell and form a brush-like surface. Since the PCNs are made up of numerous polymers we can expect them to swell greatly and in turn cover the entire underlying surface. The PCNs in the swollen state will mask the underlying surface and therefore prevent protein adhesion, in particular fibrinogen adhesion.

The nature of the PCN-coated surface will be studied using surface plasmon resonance (SPR), quartz crystal microbalance (QCM), atomic force microscopy (AFM), scanning electron

microscope (SEM), and Polarization modulation-infrared reflection adsorption spectroscopy (PM-IRRAS). Each technique offers a unique perspective on the properties of the surface. By using SPR we can monitor the adsorption of the multilayers and PCNs. AFM and SEM can then be used to see how well the PCNs cover the surface; dense surface coverage of PCNs as opposed to very bare surface with few PCNs here and there. Data collected from QCM will allow us to study the thickness and viscoelastic properties of the swollen PCNs. Lastly, PM-IRRAS can be used to analyze the surface chemistry. By themselves each technique only tells limited information about the surface but if used in conjunction with one another we can determine if we have a surface that will be suitable for blood-contacting applications; the nanoparticles swell under liquid and form a brush-like structure that covers the underlying surface.

Fibrinogen adsorption will be performed on various surfaces and then compared to see if the surface coated with PCNs is superior to other techniques. The surfaces that we will compare our PCN surface to is a surface with Hep/Tmc multilayers with either Hep or Tmc terminating layers and a surface with Hep/Chi multilayers with either Hep or Chi terminating layers. The PCN coated surfaces will be prepared with Hep/Chi and Hep/Tmc underlying multilayers with nanoparticles adsorbed on top. The expectation is that our nanoparticles coated surface will resist fibrinogen adsorption better than the other surfaces, telling us that not only is the surface chemistry important but also the nanostructure of the surface.

## CHAPTER 2

### EXPERIMENTAL SECTION

#### 2.1 MATERIALS

Chitosan (Chi) was obtained from novamatrix (Protosan UP B 90/20, 5% acetylated, Mw = 80 kDa, PDI = 1.52, Sandvika, Norway). Heparin sodium (Hep) was obtained from Celsus Laboratories (from porcine intestinal mucosa, 12.5% sulfur, Mw = 14.4 kDa, PDI = 1.14, Cincinnati, OH). *N,N,N*-Trimethyl chitosan (Tmc) was synthesized in our own lab using the procedure described by de Britto and Assis [36]. The degree of quaternization of the Tmc was determined to be 18%. 11-Mercapto-undecanoic acid (MUA) 95% and fibrinogen was purchased from Sigma-Aldrich (St. Louis, MO). Both glacial acetic acid and ethanol (200 proof 99.5 + %) were purchased from Acros Organics (Geel, Belgium). Sodium acetate anhydrous, sodium chloride, potassium chloride, and sodium phosphate dibasic anhydrous were all purchased from Mallinckrodt Chemicals (St. Louis, MO). Sodium phosphate monobasic monohydrate was purchased from Fisher Scientific (Pittsburgh, PA). SF-10 glass chips were purchased from GWC Technologies (Madison, WI). A Millipore synthesis water purification unit (Millipore, Billerica, MA) was used to obtain 18.2 M $\Omega$  cm water that was used to make all aqueous solutions.

#### 2.2 CONSTRUCTION OF HEPARIN/CHITOSAN POLYELECTROLYTE COMPLEX NANOPARTICLES.

Hep/Chi polyelectrolyte complex nanoparticles (PCN) were prepared by first making 0.95 mg/ml and 0.9 mg/ml pure polymer solutions of heparin and chitosan in acetate buffer solution (0.1 M pH 5) respectively. The solutions were allowed to stir for an hour and then filtered using 0.2  $\mu$ m syringe filters (PVDF, Fisher Scientific). Negatively charged PCNs were

prepared by using heparin as the starting solution and then adding chitosan. One part by volume chitosan was mixed into six part by volume heparin using one shot addition. The advantage of one shot addition is that it minimizes flocculation of PCNs when the charge mixing ratio is close to 1 [36]. The mixture was then allowed to stir for three hours, at which point it was turned off and left over night to settle and thus remove aggregated particles. The following day the PCN mixture was separated into small 1.5 mL Eppendorf centrifuge tubes. The solutions were then centrifuged at 9000 rcf for 15 min using an Eppendorf 5804 centrifuge (Eppendorf, Westbury, NY). After being centrifuged the supernatant was removed leaving behind the PCNs. The PCNs in each centrifuge tube were then re-suspended 150  $\mu$ L Millipore water. The PCN pellet might take a while to break down but once it does all the mixtures were combined and stored in the refrigerator. Calculating the yield of the nanoparticles is described in our previous work; it was determined to be 60% [35]. The concentration after re-suspension was calculated to be 8 mg/ml. Dynamic light scattering and zeta potential measurements were also performed according to our previous work [35]. Based on these measurements it was found that the Hep/Chi nanoparticles have an effective diameter of  $410.5 \pm 2.2$  nm, and a zeta potential of  $-51.79 \pm 0.93$  mV.

### 2.3 PREPARING THE HEP, TMC, CHI, AND FIBRINOGEN SOLUTIONS FOR CONSTRUCTION OF PEM

The PEMs were constructed using Tmc and Chi as the polycation and Hep as the polyanion. These solutions are needed to create Hep/Chi and Hep/Tmc PEMs. The chemical structure of Tmc and Chi is shown in figure 7 to emphasize the difference between Chi and Tmc. The three solutions of 0.01 M Tmc in acetate buffer (0.2 M pH 5), 0.01 M Chi in acetate buffer (0.2 M pH 5), and 0.01 M Hep in acetate buffer (0.2 M pH 5) were prepared. The solutions were



light which can be observed as a minimum in reflectivity. The position at which this minimum occurs at is called the SPR angle. The SPR angle is sensitive to the thickness and index of refraction of any adsorbed material on the metal surface [37]. By using this technique, we can detect changes in refractive index as well as thickness of the PEM on the gold surface.

The assembly of PEM was performed in a flow cell of an SPR-100 module connected to a Nicolet 8700 FT-IR spectrometer (Thermo-Electron, Madison, WI). A Masterflex peristaltic pump (Cole-Parmer, Vernon Hills, IL) set to medium speed was used to pump the rinse and polyelectrolyte solutions through the flow cell. The appropriate angle of incidence was determined by observing at what angle the minimum in reflectivity is at  $9000\text{ cm}^{-1}$  wavenumber. The configuration of the FT-SPR was as follows, a white light/near infrared source was used along with a  $\text{CaF}_2$  beam splitter at the interferometer and an InGaS detector. All of the data was collected using Omnic 8 software (Thermo Electron). The data was collected at a resolution of  $8\text{ cm}^{-1}$  over a range of  $6000$  to  $12000\text{ cm}^{-1}$ . Sixteen scans were performed at each time point and coadded to give an FT-SPR spectrum every 4.7 s.

The underlying PEM surface was prepared by using either Chi as the polycation or Tmc as the polycation and Hep as the polyanion. The procedure for creating Hep/Chi PEMs is same as that for creating Hep/Tmc PEMs so only one will be described. The Hep/Tmc PEMs were prepared by exposing the substrate to alternating solutions of Tmc and Hep for 5 min. In between each step the substrate was rinsed using the rinse solution. All the PEMs constructed contained a total of 7 layers with Tmc being the initial and final layer of the PEM. Three different substrates were prepared, a substrate that was Hep terminated and then exposed to fibrinogen, a substrate that was Tmc terminated and then exposed to fibrinogen, and a substrate that was Hep/Chi PCN

terminated and exposed to fibrinogen. The shift in position of the FT-SPR peak center of gravity can be used to determine the layer thickness [38].

## 2.5 SCANNING ELECTRON MICROSCOPY

The surface of the substrates coated with Hep/Chi nanoparticles was imaged using JEOL JSM-6500F field emission scanning electron microscope (SEM) (Jeol, Peabody, MA). The surfaces created in the FT-SPR are imaged using SEM to further analyze the distribution of nanoparticles on the surfaces of the Hep/Chi and Hep/Tmc based PEMs. Before imaging, the surface was coated with 10 nm gold using an argon atmosphere evaporator. Images were taken at 700x magnification using accelerating voltage of 5.0 kV.

## 2.6 ATOMIC FORCE MICROSCOPY

Atomic force microscopy (AFM) images of the nanoparticle terminated surface were taken using a dimension 3100 AFM microscope (Digital Instruments, Santa Barbra, CA) and Nanoscope III 4.43r8 software. The AFM was also used with the intention of studying the distribution of nanoparticles on the surfaces of Hep/Chi and Hep/Tmc based PEMs. Tap300-G Silicon AFM probes with resonant frequency of 300 kHz and force constant of 40 N/m were purchased from Ted Pella, Inc and were used for all the AFM imaging.

## 2.7 MULTILAYER ASSEMBLY USING QUARTZ CRYSTAL MICROBALANCE

Surfaces containing the PEMs and PCNs were constructed on AT-cut piezoelectric gold-coated sensor crystals (Q-Sense, Inc., Glen Burnie, MD). Before the PEMs were constructed, the substrates were soaked in 1 mM solution of MUA in ethanol for 24 hours. MUA is a good base upon which the PEMs are formed. Chi and Tmc were used as the polycation and Hep was used as the polyanion for the Hep/Chi and Hep/Tmc based PEMs. Their preparation is described in

section 2.3. The assembly of the PEMs was performed on the QCM-D crystals in a Q-sense E4 quartz crystal microbalance (QCM) with dissipation monitoring system (Q-sense, Inc.). The software used to record and analyze the data was QSoft 401 and QTools 301 (version 3.0.17.560) respectively. The flow rate used to construct the PEMs was set to 200  $\mu\text{l}/\text{min}$ . The surface was constructed with a total of 7 layers with Tmc being the initial layer and then alternating between Hep and Tmc and finally terminating with a Tmc layer. The formation of the Hep/Chi PEM is exactly the same except Chi is used instead of Tmc. In between each step a rise step is performed. The time that the surface was exposed to each polyelectrolyte varied throughout the experiment. The reason being, it took quite some time for the frequency to stabilize during each step.

### 2.7.1 KELVIN-VOIGT VISCOELASTIC MODELING FOR PCN-COATED SURFACE

QCM is a very powerful technique that allows one to characterize surface properties of thin films. Therefore, it was the logical choice in characterizing the coating of PEM and PCN process. The fundamental idea behind the QCM is that a change in the resonance frequency of the quartz crystal is correlated with the mass of the film. In particular, for films that are rigid a decrease in resonance frequency of the quartz crystal is linearly correlated with mass of the film according to the Sauerbrey model (Equation 1) [34, 39-41].

$$\Gamma_{QCM-D} = -\frac{C}{n} \Delta f_n \quad \text{Equation 2.5.1}$$

Where,  $\Gamma_{QCM-D}$  is the mass adsorbed per unit area,  $C$  ( $17.7 \text{ ng cm}^{-1}$ ) is the mass sensitivity constant,  $n$  is the overtone, and  $\Delta f_n$  is the frequency shift for overtone  $n$ . A major assumption made in the Sauerbrey model is that the adsorbed mass is evenly distributed, sufficiently rigid and has no energy dissipation. In cases where the films are viscoelastic and not rigid then this model becomes invalid because dissipation has to be taken into account in order to get an

accurate description of the films. Because we are assuming that the nanoparticles are swollen they have viscoelastic behavior and as a result we need to consider dissipation to accurately model the structural properties of the PCNs. The definition of dissipation is described as the energy loss of an oscillatory system during one period of oscillation [39]. In mathematical terms the dissipation is defined as

$$D = \frac{E_{dissipated}}{2\pi E_{stored}} \quad \text{Equation 2.5.2}$$

where  $E_{dissipated}$  is the dissipated energy,  $E_{stored}$  is stored energy in the oscillating system and  $D$  is the sum of all energy dissipated in the oscillatory system.

A more accurate model that describes viscoelastic materials is the Kelvin-Voigt model. The model is based on a dash pot-spring configuration to describe the viscoelastic properties of materials. The model is described as:

$$G^* = G' + iG'' = \mu_1 + i2\pi f\eta_1 \quad \text{Equation 2.5.3}$$

where  $G^*$  is complex shear modulus,  $G'$  is the storage modulus, and  $G''$  is the loss modulus. The Q-tool software has the ability to take the measured  $\Delta f$  and  $\Delta D$  data and interpret it based on the Kelvin-Voigt model to estimate the viscoelastic properties of the adsorbed nanoparticles. The underlying assumptions made by this model are that the film must be laterally homogenous and evenly distributed, the bulk fluid is Newtonian, the adsorbed layer couples perfectly to the sensor (no slip), and the film is soft/viscoelastic [41]. If these conditions are met then viscoelastic properties such as density, viscosity, elasticity, and thickness of the adsorbed nanoparticles can be correlated to the  $\Delta f$  and  $\Delta D$  from the QCM-D response [39]. Voinova et al. developed a mathematical relationship between the QCM-D response and the viscoelastic properties of the adsorbed film. The relationship is presented in Equation 4 and 5.

$$\Delta f \approx -\frac{1}{2\pi\rho_0 h_0} \left\{ \frac{\eta_3}{\delta_3} + \sum_{j=1,2} \left[ h_j \rho_j \omega - 2h_j \left( \frac{\eta_3}{\delta_3} \right)^2 \frac{\eta_j \omega^2}{\mu_j^2 + \omega^2 \eta_j^2} \right] \right\} \quad \text{Equation 2.5.4}$$

$$\Delta D \approx \frac{1}{2\pi f \rho_0 h_0} \left\{ \frac{\eta_3}{\delta_3} + \sum_{j=1,2} \left[ 2h_j \left( \frac{\eta_3}{\delta_3} \right)^2 \frac{\mu_j \omega}{\mu_j^2 + \omega^2 \eta_j^2} \right] \right\} \quad \text{Equation 2.5.5}$$

where  $\rho_0$  and  $h_0$  are the density and thickness of the quartz crystal.  $\eta_3$  is the viscosity of the bulk fluid and  $\delta_3$  defined as  $\delta_3 = \sqrt{2\eta_3/\rho_3\omega}$  is the viscous penetration depth of the shear wave in the bulk fluid and  $\rho_3$  is the density of the bulk fluid.  $\omega$  is the angular frequency of the oscillator. Since the QCM-D instruments can measure multiple overtones of the fundamental frequency (n=3,5,7,9,13), it can use the built-in algorithm to solve for the parameters that describe the nanoparticles: density ( $\rho_1$ ), viscosity ( $\eta_1$ ), shear elasticity ( $\mu_1$ ), and thickness ( $\delta_1$ ). In our case, since the nanoparticles are coated to a surface that already has PEMs we had to model the surface with two separate layers. Q-tools has the ability to model two separate layers with the bulk fluid being automatically the third layer. We assumed that the underlying PEM layer was a single layer, even though it is composed of seven individual layers, and the PCN was its own layer. Using the Q-tools we were able to model the surface in several different configurations (figure 8). Since there are two layers we have to provide the software with bulk fluid density and viscosity (997.62 kg/m<sup>3</sup> and 0.000933 kg/ms at 23 °C respectively). We also have to provide the density of the PEM layer and the PCN layer. We assumed that the density of these two layers is somewhere in the range of water (1000 kg/m<sup>3</sup>) and concentrated solution of Hep/Tmc (1500kg/m<sup>3</sup>).

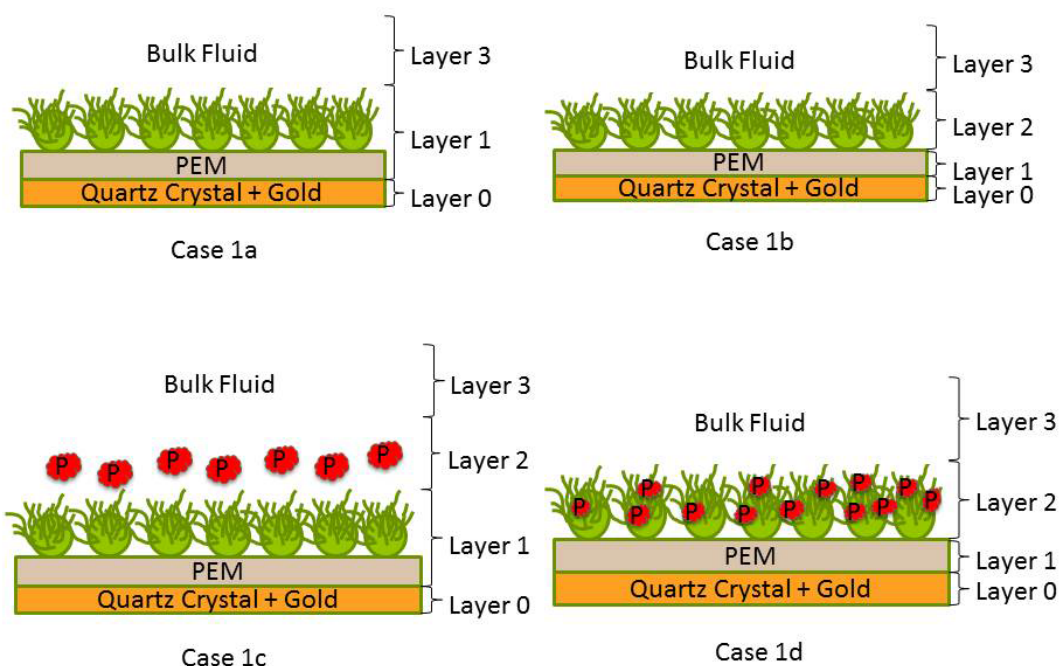


Figure 8. The various configurations that were modeled using Q-tools software. The PEM layer is composed of 7 layers of alternating Hep/Tmc monolayers, starting with Tmc and terminating with Tmc. The nanoparticles have an overall negative charge and are made using heparin in excess and chitosan as the limiting reagent. The protein used in these studies was fibrinogen.

## 2.8 POLARIZATION MODULATION-INFRARED REFLECTION ADSORPTION SPECTROSCOPY (PM-IRRAS)

Polarization modulation-infrared reflection adsorption spectroscopy (PM-IRRAS) on the surface containing the multilayers and the PCN was performed to investigate the surface chemistry. A Nicolet 8700 FT-IR Spectrometer (Thermo-Electron) configured with a Tabletop Optics module equipped with a PEM-90 photoelastic modulator (Hinds Instruments, Hillsboro, OR) to provide the polarization of the incident infrared light, a liquid nitrogen cooled MCT-A detector, and a demodulator (GWC Technologies) to process the s- and p-polarized reflection spectra [34, 36]. 1000 PM-IRRAS spectra were collected for the different surfaces at  $8 \text{ cm}^{-1}$  resolution. The PM-IRRAS was corrected using a cubic spline approximation for the background signal in IgorPro (version 5.0.5.7, Wave Metrics, Portland, OR). This was done to remove the

second-order Bessel function by dividing by a baseline. The spline-points for the baseline were chosen in regions where there were no IR adsorption peaks.

## CHAPTER 3

### RESULTS AND DISCUSSION

#### 3.1 BACKGROUND

Developing a surface that mimics the structure of the glycocalyx would be a huge breakthrough in the field of blood compatible devices. Since the glycocalyx is believed to play an essential role in preventing thrombosis, we look to it for answers. We believe that the brush-like structure is one of the key reasons for the glycoalyx having anti-thrombogenic properties. We developed a surface that we believe will have a brush-like structure, similar to the glycocalyx, using heparin (Hep)/chitosan (Chi) based nanoparticles coated onto surfaces with Hep/Trimethyl chitosan (Tmc) polyelectrolyte multilayers (PEMS). The surface morphology of the dry surface is characterized using the scanning electron microscope and atomic force microscope. We believe that under dry conditions the polyelectrolyte complex nanoparticles (PCN) are in a collapsed state but once the surface is immersed in liquids these PCNs swell and form a brush-like coating similar to the glycoalyx. The surface properties under liquid were characterized using surface plasmon resonance (SPR) and quartz crystal microbalance (QCM). The results obtained from both SPR and QCM were used in conjunction to see whether or not our original hypothesis that the nanoparticles swell up and form a brush-like surface similar to the glycocalyx was correct.

#### 3.2 FORMATION OF PEMS AND PCN-COATED SURFACE USING SPR

The plot showing the formation of the Hep/Tmc PEMS containing negatively charged Hep/Chi PCNs was monitored using SPR. The SPR data for the formation of Hep/Chi PEMS is not presented because it was later observed that Hep/Chi PEMS do not adsorb nanoparticles as well as Hep/Tmc PEMS, this will be discussed in further detail in section 3.3. The formation of

the surface is shown in the FT-SPR time series in figure 9. For the first five minutes the surface was exposed to acidified rinse. After the initial acidified rinse the surface is exposed to Tmc solution at which point we see a shift in the peak position indicating a change in refractive index from the acidified rinse to the Tmc solution. Once the solution is switched back to the acidified rinse we see that the peak shift back up because now the refractive index changes from the Tmc solution to that of the acidified rinse. The peak position not going back to its original position is an indication that there is adsorption of multilayers. The adsorption process for the Hep-terminated and Tmc-terminated is shown in figure 10, from this we can see the adsorption of the PEMs as well as some adsorption of fibrinogen. The model calculates the thickness of each layer by using multiphase Fresnel calculations to predict the FT-SPR peak for an array of thicknesses. This requires knowing thickness of the gold layer (45 nm) as well as the refractive index of SF-10 glass, gold, PEM, and rinse solutions. The refractive index of the PEM solutions was calculated using ellipsometry in our previous work [36]. The algorithm was based on a script created by Prof. Robert Corn from the University of California, Irvine. A detailed analysis of this procedure can be found in the sporting information of previous work done in our lab [36]. By fixing the angle of incidence to  $51.2^\circ$  as well as the refractive index of all the solutions, the only adjustable parameter is the thickness of the PEM.

The FT-SPR curves were predicted using the algorithm with the thickness being the independent variable. Using this technique we were able to determine the thickness for each surface we created, heparin terminated and Tmc terminated in figure 10 while PCN terminated on table 2. As can be seen on this table the thickness of the seven underlying PEMs is approximately  $6.20 \pm 0.15$  nm. These results agree with previous work done in our lab, in which we also found that the height of seven layers composed of Tmc and Hep is approximately 6 nm.

The thickness of the eighth layer is not what we expected, because we assumed that the refractive index of the PCN layer is the same as that of the Hep/Tmc layers. Another explanation for the PCN layer having such a small thickness could be attributed to the SPR not being able to measure this layer properly. We assumed that when the surface is exposed to liquid, the nanoparticles swell and form a brush-like structure. As a result of swelling the nanoparticles absorb a lot of water. As mentioned in chapter 2, the SPR is sensitive to refractive index contrast. If the nanoparticles are severely hydrated then they will have a similar refractive index to that of water. As a result, there is no contrast and the PCN layer cannot be accurately measured. It should be noted that the data presented in table 2 is calculated using the model based on the assumption that the nanoparticle layer has the same refractive index as that of the PEM layer. This assumption is not accurate if the nanoparticles are hydrated which they might be in our case. Even though the SPR cannot measure the thickness, it still can tell us whether or not the nanoparticles adsorbed on to the surface. In our case they did, and this was later confirmed using SEM and AFM imaging.

The model that we used to predict the FT-SPR curves is based on the theory developed by Wilford Hansen [42]. The model he developed for predicting the FT-SPR curves is based on the assumption that there are three phases. In our case the three phases are the gold film, the PEM film, and the prism. We could add a fourth phase for the PCN layer to account for the fact that it has a different refractive index than the PEM layer, but this requires us to make the assumption that the interfaces between layers are smooth and discrete which may not be the case. We relied on the SPR to confirm that the nanoparticles had deposited on to the surface and then confirmed using SEM and AFM imaging. Instead of using SPR we used QCM in the hopes that it will be better able to characterize the PCN-coated surface.

Table 2. Thickness of the PEM surface, layers 1-7 are composed of Heparin and Tmc. The first and seventh layers are Tmc layers. The eighth layer is the Hep/Chi PCN layer assuming that it has the same refractive index as the polyelectrolyte solutions.

Layer	Thickness (nm)
1	$0.70 \pm 0.04$
2	$1.03 \pm 0.00$
3	$1.30 \pm 0.20$
4	$1.60 \pm 0.04$
5	$2.40 \pm 0.05$
6	$3.10 \pm 0.00$
7	$5.04 \pm 0.10$
8	$6.20 \pm 0.15$

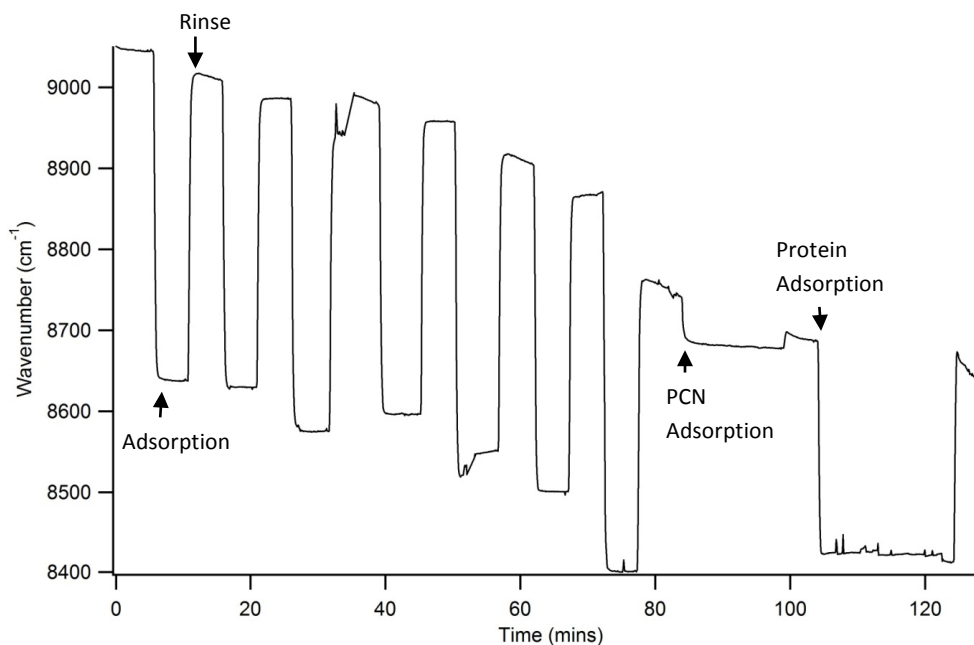


Figure 9. The SPR time series for a surface containing 7 monolayers composed of alternating Hep/Tmc layers, the initial and final layers both being Tmc. The arrows indicate the start of the adsorption and rinse steps respectively. After the 7th layer the surface is exposed to negatively charged Hep/Chi nanoparticles. Once the nanoparticles are adsorbed the surface is finally exposed to fibrinogen.

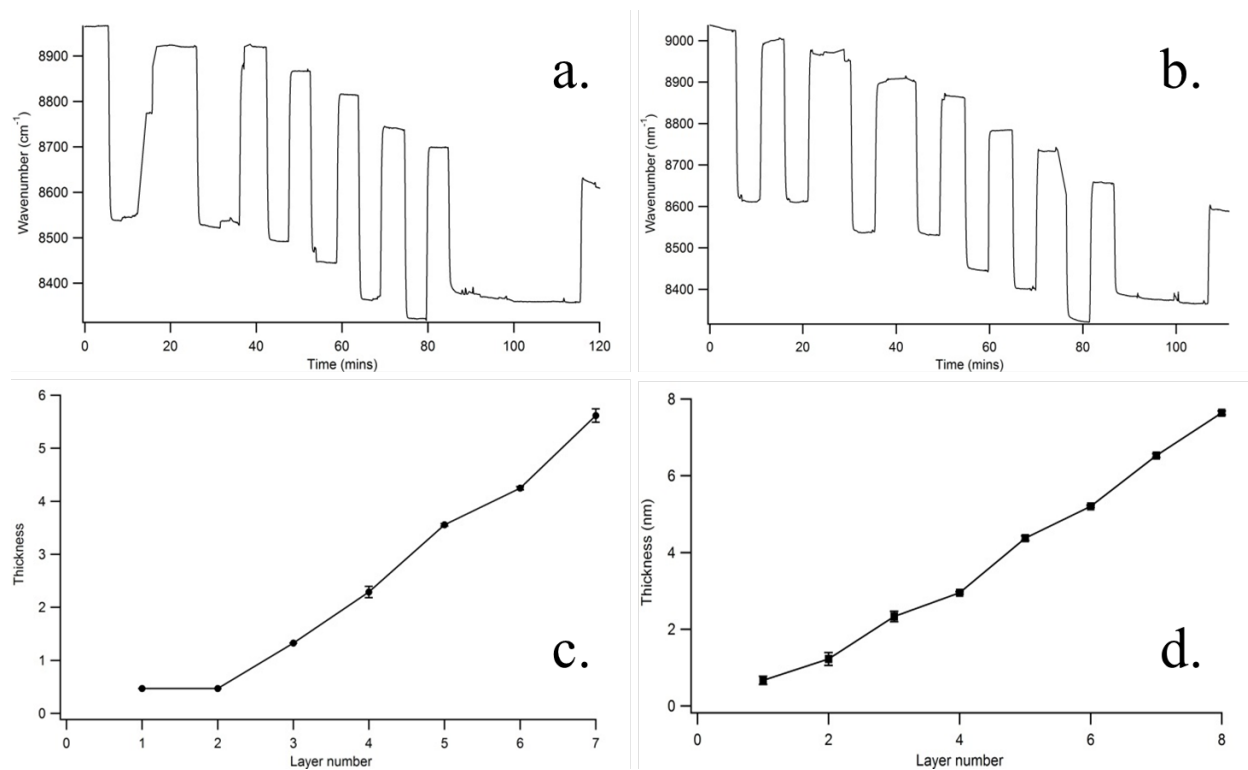


Figure 10. The SPR results for a heparin terminated surface (a) exposed to fibrinogen and a Tmc terminated surface (b) exposed to fibrinogen. The thickness for a heparin terminated surface (c) exposed to fibrinogen and a Tmc terminated surface (d) exposed to fibrinogen using Fresnel calculations.

### 3.3 SURFACE MORPHOLOGY

The surfaces prepared in the SPR flow cell was imaged using AFM as well as SEM. AFM and SEM were used to study the features of the surface after the deposition of the nanoparticles. The AFM and SEM images are shown in figure 11. Based on these images we can see that the nanoparticles were deposited onto the surface of the Hep/Tmc PEMs but are hardly deposited on the Hep/Chi PEMs. Several attempts were made to adsorb Hep/Chi PCNs onto Hep/Chi PEMs but were not successful. For example, the layers onto which the nanoparticles adsorb was increased but this did not solve the problem. Using nanoparticles with a higher negative charge was also attempted but was unsuccessful. The nanoparticles not adsorbing on to the Hep/Chi PEMs might be because the terminating chitosan layer does not interact as strongly with the PCNs as does the Tmc layer on the Hep/Tmc PEMs. From the SEM images we can see

how much better the adsorption of the PCNs is on the Hep/Tmc PEMs compared to the Hep/Chi PEMs. Since Tmc is more positively charged than Chi we see that the nanoparticles are somewhat collapsed on the surface and there is uniform coverage on the surface. These results prompted us to abandon Hep/Chi PEMs and focus on only using Hep/Tmc PEMs for all further studies.

The pair of AFM and SEM images are of the same surface for the Hep/Tmc PEMs and Hep/Chi PEMs. The AFM images were taken prior to the SEM images to avoid imaging the surface with an extra layer of gold which is required for the SEM image. Images of nanoparticles adsorbed onto the surface of Hep/Tmc PEMs are in agreement with one another, they both show that the nanoparticles are on the order of 500 nm. The AFM also measures the height of the surface, not shown in figure 11, but from the AFM it was determined that the height of the nanoparticles was on the order of 30 nm. It should be noted that these images show the morphology of the surface under a dry state. This is not exactly what we were after; we want to see if they swell after being immersed in liquid buffer such as PBS. From image (a) we can see that the nanoparticles seem to be collapsed on the surface, this can be a result of the strong interaction between negatively charged nanoparticles and the positively charged Tmc monolayer. Both images also confirm that there is a uniform coverage of the surface. This is crucial if this technique is to have any application in blood-contacting surfaces. If underlying surface is exposed then there is a possibility of platelet adhesion which can further lead to clotting. Since the surface is uniformly covered we expect that once the surface is immersed in buffer that the nanoparticles swell up and therefore completely cover the underlying surface.

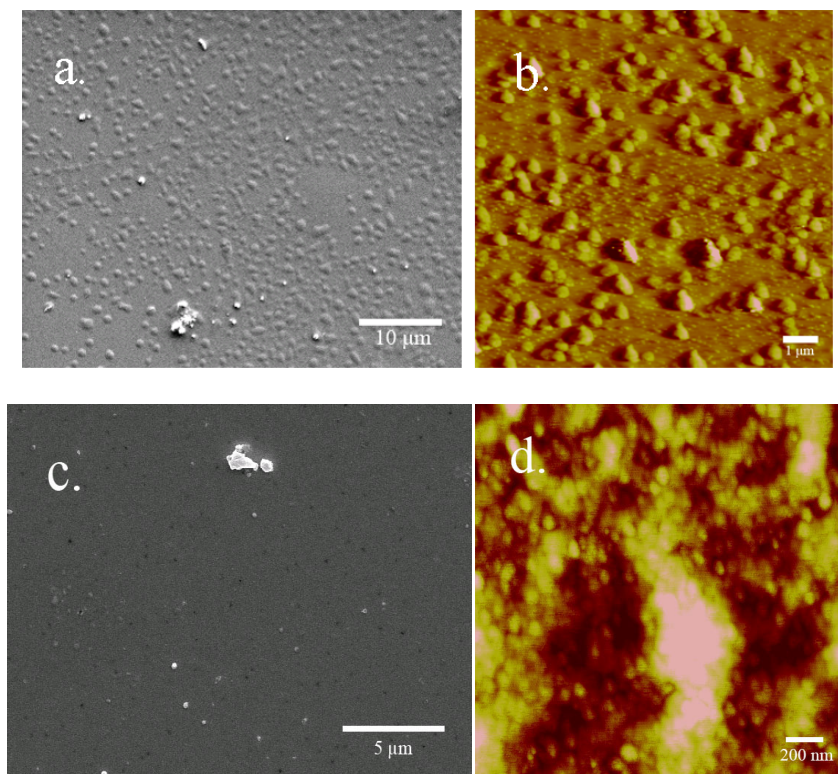


Figure 11. SEM (a) and AFM (b) images of the negatively charged Hep/Chi nanoparticles on Hep/Tmc based PEMs. Both of these images confirm the deposition of nanoparticles on to the surface. SEM (c) and AFM (d) images of negatively charged Hep/Chi nanoparticles on Hep/Chi based PEMs. When Hep/Chi PEMs were used we observed that there was no adsorption of nanoparticles on Hep/Chi based PEMs. Unlike SPR where the size of the nanoparticles is difficult to determine, with SEM and AFM the size of the nanoparticles is approximately 500 nm. The top set of images are of the same surface as are the bottom, AFM was done before SEM.

### 3.4 SURFACE CHEMISTRY

PM-IRRAS was also performed before the surfaces were prepared for SEM. Three different surfaces that were exposed to fibrinogen were analyzed: Hep-terminated, Tmc-terminated, and PCN-terminated. Surfaces without protein were also analyzed for comparison. The goal was to see if the coated surfaces were able to resist fibrinogen adhesion. The PM-IRRAS spectra for the six surfaces is presented in figure 12. A complete analysis of peak assignment for Hep/Tmc PEMs is covered in previous work done in the lab [36]. From these spectra we can definitely confirm that these are Hep/Tmc PEMs. There is a characteristic peak at  $1252\text{ cm}^{-1}$  due to the asymmetric stretching of sulfate groups on the Hep. It should also be noted that this peak also seems to increase in the PCN layer due to the increase in sulfate groups

present in the Hep/Chi nanoparticles. From the Tmc-terminated layer we can see that there are two strong peaks at  $1620\text{ cm}^{-1}$  and  $1680\text{ cm}^{-1}$ . These peaks are result of carbonyl stretching in the protein backbone and other modes of stretching in the protein. These two peaks are very distinct in the Tmc layer whereas on the Hep and PCN layers there is a broad peak which seems to have smaller peaks. This peak present from  $1700 - 1600\text{ cm}^{-1}$  was also present in previous spectra taken in our lab. This broad absorption peak is characteristic of asymmetric stretch of the amide carbonyl groups.

Since we collected the spectra for both types of surfaces, with and without protein, we were able to perform a calculation that allowed us to see if protein had adsorbed on to the surface. We performed this simple calculation by normalizing each spectrum with its total area from 1000 to 2000 wavenumbers and then taking the difference between the adsorbed surface and the protein free surface to obtain the difference. From this difference we can tell weather protein adsorbed or not. From figure 12 we can see from the spectra of the Tmc-terminated surface that there are lots of changes upon protein adsorption indicating lots of fibrinogen adsorbed. The Hep-terminated and PCN-Terminated spectra show that there is very little change upon protein adsorption indicating very little change in chemistry. This is also confirmed by the difference curves, we can see that both the Hep-terminated and PCN-terminated curves are featureless compared to the Tmc-terminated surface. From this we can conclude that Tmc-terminated layers adsorbed fibrinogen whereas Hep and PCN layers are resistant to its adsorption.

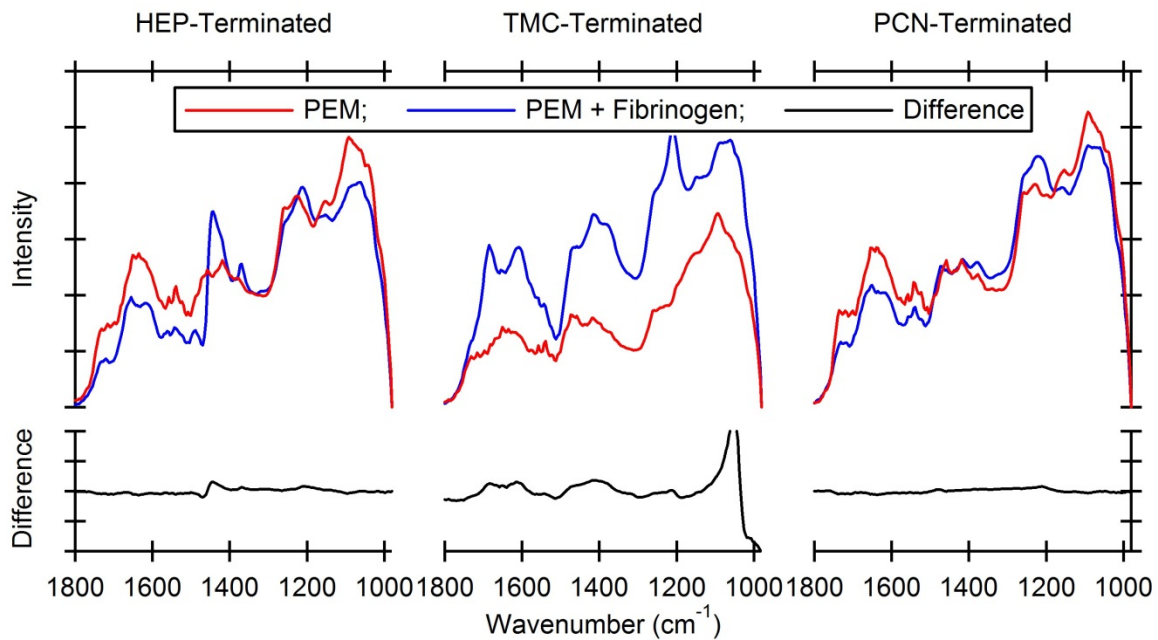


Figure 12. The PM-IRRAS spectra for Hep-terminated PEM with (blue) and without (red) fibrinogen, Tmc-terminated PEM with (blue) and without (red) fibrinogen, and PCN-terminated with (blue) and without (red) fibrinogen. The difference between the spectra was taken to see if protein had adsorbed to surfaces that were exposed to protein. Based on the difference we can see that Hep-terminated and PCN-terminated have no protein adsorption since the spectra are same before and after protein adsorption. The difference for the Tmc-terminated shows that fibrinogen had adsorbed to that surface.

### 3.5 FORMATION OF PEMS AND PCN-COATED SURFACE USING QCM

The surfaces were also prepared using QCM, with this technique we can monitor the deposition of PEMS and PCN by monitoring shift in frequencies. We can then determine the thickness, viscosity, and sheer modulus of the surface under liquid conditions, something that we were not able to do using SPR. As mentioned earlier, Kelvin-Voigt model is used to solve for thickness, viscosity, and sheer modulus. For this model to give an accurate description of the surface there are few key assumptions made: the film must be laterally homogenous and evenly distributed, the bulk fluid is Newtonian, the adsorbed layer couples perfectly to the sensor (no slip), and the film is soft/viscoelastic. A surface containing Hep/Tmc PEMS and Hep/Chi PCN was prepared, the overtones  $n = 3, 5, 7, 9, 11, 13$  were measured as a function of time. It should be noted that QCM was only used to analyze PCN adsorption onto Hep/Tmc PEMS and not Hep/Chi PEMS. As mentioned in section 3.3, once we observed that Hep/Chi based PEMS were poor at adsorbing the PCNs we decided to only use Hep/Tmc PEMS for further studies. The adsorption of the PEMS and PCNs process using the QCM is shown in figure 13. Just based on the frequency data we can tell a little bit about the nature of the surface. The first seven layers seem to be stiff since the frequency shifts are all close to one another. After the adsorption of the PCN layer we observe that the overtones segregate indicating that we might have a softer layer. The shift in frequency is an indication of mass adsorption. We observe that once fibrinogen is added (after 250 minutes) and a rinse step is done, the frequency shift goes above the previous step. This is an indicative of loss of mass. This might be due to fibrinogen binding to the nanoparticles and displacing water. It should also be noted that dissipation data was also measured but was excluded when using the model to calculate sheer modulus, viscosity, and thickness. This was done because the dissipation data contained a lot of noise preventing

acceptable fit of the model when included. Therefore only  $n = 5, 7, 9, 13$  overtones were used to calculate the shear modulus, viscosity and thickness of the layers.

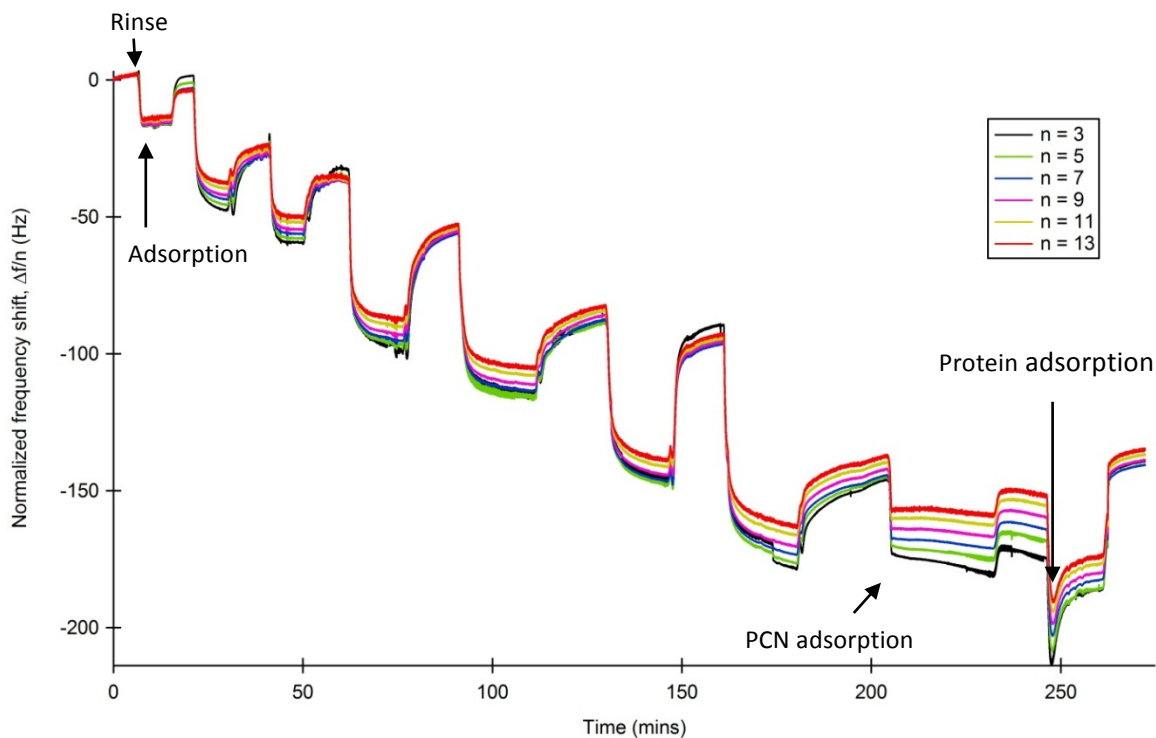


Figure 13. The adsorption of PEMs and PCNs using QCM. This shows the adsorption of 7 multilayers followed by the adsorption of PCNs and then finally fibrinogen. The arrows indicate the start of adsorption and rinse steps respectively. As can be seen from the frequency, the layers seem to be stiff up until the 7 layer. Once the PCN layer is added we see a split in the frequency which is characteristic of more viscous layers.

Using the Q-tools software we were able to determine the the thickness, viscosity, and shear modulus of our surfaces for the various cases mentioned. The results for these various cases is presented table 3. From Q-tools using the Kelvin-Voight model we determine that the underlying PEM layer has a thickness of  $19.0 \pm 0.08$  nm thickness. Once the properties of the underlying PEM were determined it was lumped into one layer for futher calculations, meaning that the properties of the seventh layer defines the entire PEM layer. Q-tools has the ability to calculate the properites of two-layer systems with the quartz and bulk layer being already taken into account as the third and fourth layers. This gave us the flexibility to try different combinations of how we thought the layers might be coupled. In the first combination we

assumed that the PEM layer and PCN layer was one layer. By making this assumption we are treating both of these layers as the same, meaning that they are both viscous or very stiff. This might not be the case in reality. By making this assumption we see that the thickness of this layer is  $31.5 \pm 0.6$  nm, the shear modulus is  $0.03 \pm 0.02$  MPa, and the viscosity is  $2.2 \pm 0.1$  cP. The thickness of the entire layer seems to be quite small, this might be because we are assuming that the PEM layer and the PCN both have the same mechanical properties, when in reality they might have completely different properties. It should be noted that when calculating these properties we assumed that the density of the PEM layer was  $1400 \text{ kg/m}^3$ . This was done because we expect the density of the polysaccharide solutions to be between that of water ( $1000 \text{ kg/m}^3$ ) and a very concentrated solution of polysaccharides ( $1500 \text{ kg/m}^3$ ). When the density was varied from  $1000 \text{ kg/m}^3$  to  $1500 \text{ kg/m}^3$ , it was observed that a density of  $1400 \text{ kg/m}^3$  gave the best fit.

Even though we modeled various cases, only a few of them make physical sense. For example, from case 1b we see that the thickness of the nanoparticles layer is  $70.0 \pm 13$  nm. This result is very similar to the result we obtained from AFM. Using the AFM we were able to determine that the height of the nanoparticles on the surface was approximately 30 nm in the dry state. Therefore the thickness of  $70.0 \pm 13$  nm physically makes sense since we expect the nanoparticles to swell. For some of the other cases, the reason that the QCM might not be giving us better results is because in our original model we assumed that the nanoparticles are uniformly distributed over the surface and they are coupled to the underlying surface. We believe that the nanoparticles might not be completely coupled to the surface. The vibrating crystal might be preventing the PCNs from coupling to the surface, thus giving an inaccurate description of the surface properties. But based on the SEM and AFM images we are confident that we have a surface that behaves like a brush when under fluid. Again, even though we were

able to use the model to calculate the properties of case 1a and case 1c we do not believe they provide any valuable information, they were done for the sake of completeness. The PEM and PCN layers have completely different properties therefore combining them into one layer does not give an accurate description of that layer. We expect the PCNs to be highly hydrated therefore their viscosity should be close to that of water. But what we observe from the QCM is that the viscosity of case 1b is lower than that of water. Again this might all go back to the nanoparticles not being completely coupled to the surface. Therefore, we are not getting an accurate description of the surface properties.

One thing we do observe is that we are definitely getting PEM formation and PCN adsorption. We can compare the thickness obtained from QCM and the peak shift from the SPR in figure 14. From this plot we see that after the adsorption of PCNs at layer 7 we see that in the SPR plot that there is a slight peak position whereas in the QCM data we see a huge increase in thickness. This shows that we definitely have PCNs that are on the surface but we just weren't able to accurately obtain that thickness using SPR. This is because SPR determines the thickness based on changes in refractive indices. If the nanoparticles are highly hydrated then they will have a refractive index close to that of water. If the refractive index of the rinse solution and the PCN solutions are very similar then we expect the peak not to shift by that much. This results in us not being able to measure the thickness of this particular layer. That is why we resort to using the QCM.

Even though case 1a and 1c are not very useful, case 1d might tell us somewhat of the interaction between the nanoparticles and the fibrinogen. From case 1b we see that the thickness of the nanoparticles before fibrinogen adsorption is  $70.0 \pm 13$  nm. Once we expose the surface to fibrinogen and treat the nanoparticle and fibrinogen layer as one layer we see from case 1d that

this layer has a thickness of  $26.0 \pm 2.0$  nm. This might indicate that the nanoparticles collapse once exposed to fibrinogen as a result of fibrinogen displacing the water.

Though the QCM results are positive we did not expect to get some of the values that we did. Most of the results obtained for the thickness make physical sense but the results for the shear modulus and viscosity are not what we were expecting. To use the Kelvin-Voigt model, it was assumed that the film is completely coupled to the surface. In reality this might not be true, therefore we are not getting a true representation of the shear modulus and viscosity of the surface. If the nanoparticles are hydrated we were expecting the surface to have a viscosity close to that of water but instead we get values that are much lower in comparison. Same for the shear modulus, we were expecting much larger values but instead the values are very small. This all goes back to the nanoparticles possibly not being coupled to the surface. If we can somehow create conditions in which the nanoparticles are able to couple with the underlying surface we might get results that are significantly better. Also, we ignored the dissipation data when calculating all the quantities in table 3 because it was noisy and prevented an acceptable fit of the model. Again the dissipation data might have been noisy because of the PCNs not being completely coupled to the surface.

Table 3. The thickness, viscosity, and shear modulus for the cases presented in figure 8. These values were obtained from Q-tools using the Kelvin-Voigt model. The thickness, viscosity, and shear modulus of each monolayer in the PEM was also determined.

	$h_1$ (nm)	$\mu_1$ (MPa)	$\eta_1$ (cP)	$h_2$ (nm)	$\mu_2$ (MPa)	$\eta_2$ (cP)
<b>Layer</b>	<b>PEM Layer</b>					
3	$4.60 \pm 0.05$	$0.26 \pm 0.01$	$2.7E-7 \pm 2.0E-8$			
4	$7.4 \pm 0.1$	$1.1 \pm 0.3$	$1.4 \pm 0.8$			
5	$11.7 \pm 0.1$	$1.5 \pm 0.1$	$4.0 \pm 1.0$			
6	$12.5 \pm 0.1$	$1.8 \pm 0.4$	$2.0 \pm 1.0$			
7	$19.0 \pm 0.1$	$1.9 \pm 0.1$	$5.0 \pm 0.6$			
<b>Naoparticle and Protein layer</b>						
Case 1a				$31.5 \pm 0.6$	$0.03 \pm 0.02$	$2.2 \pm 0.1$
Case 1b	$19.0 \pm 0.1$	$1.9 \pm 0.1$	$5.0 \pm 0.6$	$70.0 \pm 13$	$0.01 \pm 0.0015$	$0.75 \pm 0.02$
Case 1c	$31.5 \pm 0.6$	$0.03 \pm 0.02$	$2.2 \pm 0.1$	$1.70 \pm 0.05$	$0.0100 \pm 0.0002$	$0.16 \pm 0.003$
Case 1d	$19.0 \pm 0.1$	$1.9 \pm 0.1$	$5.0 \pm 0.6$	$26.0 \pm 2.0$	$0.010 \pm 0.002$	$0.600 \pm 0.003$

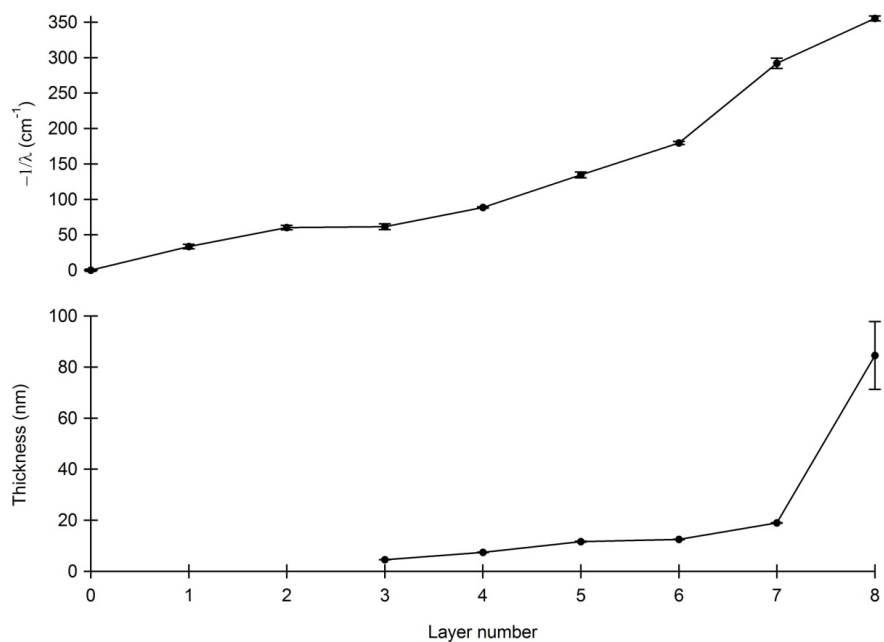


Figure 14. The adsorption of the PEMs using SPR (top) and the thickness of the PEMs using QCM (bottom). The top plot shows the average shift in peak position and the bottom shows the average thickness. From this plots we can see that there is PCN deposition on the surface (layer number 8). In SPR there is a slight shift in peak position that somewhat confirms there is PCN deposition. With QCM we can clearly see that the PCNs are adsorbed to the surface based on the thickness.

## CHAPTER 4

### CONCLUSION

#### 4.1 CONCLUSION

In this work, we developed and characterized a surface based on polysaccharide based polyelectrolyte multilayers (PEM) and polyelectrolyte complex nanoparticles (PCN). By adsorbing PCNs onto the surface we have a surface that has brush-like features that are similar to those found on the luminal surface of blood vessels. From atomic force microscopy (AFM) and scanning electron microscope (SEM) we analyze the nanoscale features of the surface. From these techniques we see that the surface has a uniform coverage of PCNs that are approximately 400 nm in diameter and 20-30 nm in height in dry conditions. Using quartz crystal microbalance (QCM) and surface plasmon resonance (SPR) we were able to study the properties of the surface when immersed in liquid. From these studies we concluded that under fluid conditions the PCNs do in fact swell up like we had originally hypothesized. From our preliminary work regarding fibrinogen adhesion we were not able to draw direct conclusion on the ability of the surface to resist protein adhesion. Combining all the results from all the techniques, we are confident that we have a surface that has a dense brush-like structure when immersed in liquid. These surfaces should be further evaluated to determine their blood compatibility to determine their suitability for blood-contacting applications.

## REFERENCES

- [1] Zhu DM, Fang JJ, Wu B, Du XB. Viscoelastic response and profile of adsorbed molecules probed by quartz crystal microbalance. *Physical Review E*. 2008;77:7.
- [2] Ratner BD. The catastrophe revisited: Blood compatibility in the 21st century. *Biomaterials*. 2007;28:5144-7.
- [3] Lamba NMK, Baumgartner JN, Cooper SL. The influence of thrombus components in mediating bacterial adhesion to biomaterials. *Journal of Biomaterials Science-Polymer Edition*. 2000;11:1227-37.
- [4] Tassiopoulos AK, Greisler HP. Angiogenic mechanisms of endothelialization of cardiovascular implants: a review of recent investigative strategies. *Journal of Biomaterials Science-Polymer Edition*. 2000;11:1275-84.
- [5] Yu K, Lai BFL, Kizhakkedathu JN. Carbohydrate Structure Dependent Hemocompatibility of Biomimetic Functional Polymer Brushes on Surfaces. *Advanced Healthcare Materials*. 2012;1:199-213.
- [6] Reitsma S, Slaaf DW, Vink H, van Zandvoort M, Egbrink M. The endothelial glycocalyx: composition, functions, and visualization. *Pflugers Archiv-European Journal of Physiology*. 2007;454:345-59.
- [7] Brash JL. Exploiting the current paradigm of blood-material interactions for the rational design of blood-compatible materials. *Journal of Biomaterials Science-Polymer Edition*. 2000;11:1135-46.
- [8] Li S, Henry JJD. Nonthrombogenic Approaches to Cardiovascular Bioengineering. In: Yarmush ML, Duncan JS, Gray ML, editors. *Annual Review of Biomedical Engineering*, Vol 13. Palo Alto: Annual Reviews; 2011. p. 451-75.
- [9] Jung F, Braune S, Lendlein A. Haemocompatibility testing of biomaterials using human platelets. *Clinical Hemorheology and Microcirculation*. 2013;53:97-115.
- [10] Sen Gupta A, Wang S, Link E, Anderson EH, Hofmann C, Lewandowski J, et al. Glycocalyx-mimetic dextran-modified poly(vinyl amine) surfactant coating reduces platelet adhesion on medical-grade polycarbonate surface. *Biomaterials*. 2006;27:3084-95.
- [11] Werner C, Maitz MF, Sperling C. Current strategies towards hemocompatible coatings. *Journal of Materials Chemistry*. 2007;17:3376-84.
- [12] Nieuwdorp M, Meuwese MC, Vink H, Hoekstra JBL, Kastelein JJP, Stroes ESG. The endothelial glycocalyx: a potential barrier between health and vascular disease. *Current Opinion in Lipidology*. 2005;16:507-11.
- [13] Secomb TW, Hsu R, Pries AR. Effect of the endothelial surface layer on transmission of fluid shear stress to endothelial cells. *Biorheology*. 2001;38:143-50.
- [14] Barrientos AG, de la Fuente JM, Rojas TC, Fernandez A, Penades S. Gold glyconanoparticles: Synthetic polyvalent ligands mimicking glycocalyx-like surfaces as tools for glycobiological studies. *Chemistry-a European Journal*. 2003;9:1909-21.
- [15] Bosker WTE, Patzsch K, Stuart MAC, Norde W. Sweet brushes and dirty proteins. *Soft Matter*. 2007;3:754-62.
- [16] Parnell AJ, Martin SJ, Jones RAL, Vasilev C, Crook CJ, Ryan AJ. Direct visualization of the real time swelling and collapse of a poly(methacrylic acid) brush using atomic force microscopy. *Soft Matter*. 2009;5:296-9.

- [17] Sui XF, Zapotoczny S, Benetti EM, Schon P, Vancso GJ. Characterization and molecular engineering of surface-grafted polymer brushes across the length scales by atomic force microscopy. *Journal of Materials Chemistry*. 2010;20:4981-93.
- [18] Vladkova TG. Surface Engineered Polymeric Biomaterials with Improved Biocontact Properties. *International Journal of Polymer Science*. 2010.
- [19] Pries AR, Secomb TW, Gaehtgens P. The endothelial surface layer. *Pflugers Archiv-European Journal of Physiology*. 2000;440:653-66.
- [20] Boddohi S, Kipper MJ. Engineering Nanoassemblies of Polysaccharides. *Advanced Materials*. 2010;22:2998-3016.
- [21] Biomaterials science an introduction to materials in medicine. San Diego: Academic Press; 1996.
- [22] Ly M, Laremore TN, Linhardt RJ. Proteoglycomics: Recent Progress and Future Challenges. *Omics-a Journal of Integrative Biology*. 2010;14:389-99.
- [23] Malavaki CJ, Theocharis AD, Lamari FN, Kanakis I, Tsegenidis T, Tzanakakis GN, et al. Heparan sulfate: biological significance, tools for biochemical analysis and structural characterization. *Biomedical Chromatography*. 2011;25:11-20.
- [24] Olson ST, Bjork I. REGULATION OF THROMBIN ACTIVITY BY ANTITHROMBIN AND HEPARIN. *Seminars in Thrombosis and Hemostasis*. 1994;20:373-409.
- [25] Wu KK, Thiagarajan P. Role of endothelium in thrombosis and hemostasis. *Annual Review of Medicine*. 1996;47:315-31.
- [26] Bedsted T, Swanson R, Chuang YJ, Bock PE, Bjork I, Olson ST. Heparin and calcium ions dramatically enhance antithrombin reactivity with factor IXa by generating new interaction exosites. *Biochemistry*. 2003;42:8143-52.
- [27] Dalainas I, Avgerinos ED, Liapis CD. Heparin-induced thrombocytopenia: what a vascular surgeon needs to know. *Journal of Cardiovascular Surgery*. 2011;52:81-8.
- [28] Lagergre.H, Olsson P, Swedenbo.J. INHIBITED PLATELET ADHESION - NON-THROMBOGENIC CHARACTERISTIC OF A HEPARIN-COATED SURFACE. *Surgery*. 1974;75:643-50.
- [29] Yoon JH, Jang IK. Heparin-Induced Thrombocytopenia in Cardiovascular Patients Pathophysiology, Diagnosis, and Treatment. *Cardiology in Review*. 2011;19:143-53.
- [30] Olsson P, Lagergren H, Larsson R, Radegran K. PREVENTION OF PLATELET-ADHESION AND AGGREGATION BY A GLUTARDIALDEHYDE-STABILIZED HEPARIN SURFACE. *Thrombosis and Haemostasis*. 1977;37:274-82.
- [31] Jaax ME, Greinacher A. Management of heparin-induced thrombocytopenia. *Expert Opinion on Pharmacotherapy*. 2012;13:987-1006.
- [32] Otis SA, Zehnder JL. Heparin-induced thrombocytopenia: Current status and diagnostic challenges. *American Journal of Hematology*. 2010;85:700-6.
- [33] Chen JL, Li QL, Chen JY, Chen C, Huang N. Improving blood-compatibility of titanium by coating collagen-heparin multilayers. *Applied Surface Science*. 2009;255:6894-900.
- [34] Boddohi S, Almodovar J, Zhang H, Johnson PA, Kipper MJ. Layer-by-layer assembly of polysaccharide-based nanostructured surfaces containing polyelectrolyte complex nanoparticles. *Colloids and Surfaces B-Biointerfaces*. 2010;77:60-8.
- [35] Boddohi S, Moore N, Johnson PA, Kipper MJ. Polysaccharide-Based Polyelectrolyte Complex Nanoparticles from Chitosan, Heparin, and Hyaluronan. *Biomacromolecules*. 2009;10:1402-9.

- [36] Almodovar J, Place LW, Gogolski J, Erickson K, Kipper MJ. Layer-by-Layer Assembly of Polysaccharide-Based Polyelectrolyte Multilayers: A Spectroscopic Study of Hydrophilicity, Composition, and Ion Pairing. *Biomacromolecules*. 2011;12:2755-65.
- [37] Frutos AG, Weibel SC, Corn RM. Near-infrared surface plasmon resonance measurements of ultrathin films. 2. Fourier transform SPR spectroscopy. *Analytical Chemistry*. 1999;71:3935-40.
- [38] Boddohi S, Killingsworth CE, Kipper MJ. Polyelectrolyte multilayer assembly as a function of pH and ionic strength using the polysaccharides chitosan and heparin. *Biomacromolecules*. 2008;9:2021-8.
- [39] Liu SX, Kim JT. Application of Kelvin-Voigt Model in Quantifying Whey Protein Adsorption on Polyethersulfone Using QCM-D. *Jala*. 2009;14:213-20.
- [40] Alves NM, Picart C, Mano JF. Self Assembling and Crosslinking of Polyelectrolyte Multilayer Films of Chitosan and Alginate Studied by QCM and IR Spectroscopy. *Macromolecular Bioscience*. 2009;9:776-85.
- [41] Voinova MV, Rodahl M, Jonson M, Kasemo B. Viscoelastic acoustic response of layered polymer films at fluid-solid interfaces: Continuum mechanics approach. *Physica Scripta*. 1999;59:391-6.
- [42] Hansen WN. ELECTRIC FIELDS PRODUCED BY PROPAGATION OF PLANE COHERENT ELECTROMAGNETIC RADIATION IN A STRATIFIED MEDIUM. *Journal of the Optical Society of America*. 1968;58:380-&.